ACS APPLIED MATERIALS & INTERFACES

Letter

www.acsami.org

Plasmonic Photosensitization of Polyaniline Prepared by a Novel Process for High-Performance Flexible Photodetector

Tapan Barman and Arup R. Pal*

Physical Sciences Division, Institute of Advanced Study in Science and Technology, Paschim Boragaon, Garchuk, Guwahati 781035, Assam, India

Supporting Information

ABSTRACT: We report the synthesis of a polyaniline (PAni)−gold nanoparticle (AuNP) composite thin film in a single step. A flexible high-performance visible photodetector is constructed using PAni−AuNP composite with low loading of AuNP, and optoelectronic properties of the device are evaluated. The present study demonstrates that a plasmonic hybrid nanocomposite prepared by a single-step novel plasma-based dry process could solve the low lifetime and performance-related issues of organic optoelectronic devices.

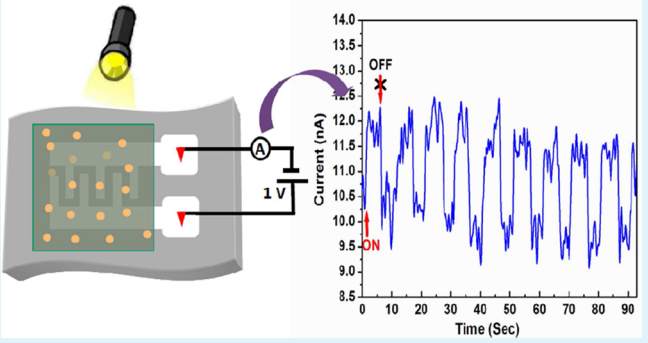

KEYWORDS: *nanocomposite materials, surface plasmon, photosensitization, photodetector*

Polyaniline is most extensively studied among the conducting polymer family because of its interesting electronic and optical properties.[1−5] The half oxidized emerldine form of polyaniline is intrinsically a p-type wide band gap semiconductor and its conductivity varies with the synthesis routes.[2,3] Composite forms of polyaniline with different organic or inorganic nanostructures attract more attention due to their interesting properties which are unattainable in pure polyaniline.[6−8] Polyaniline in pure and composite form is successfully applied in different nanostructured device realizations.[6−9] Among all the devices, organic photovoltaics and photodetectors have received considerable attention as they are related to green energy harvesting with flexible architectures.[6−8] One strategy of improving light harvesting ability of wide band gap organic semiconductor is to dope or photosensitize by photons of sub band gap energies.[10] Photosensitization of wide band gap semiconductor is possible in a number of ways.[6−8] Plasmonic photosensitization of wide band gap semiconductor is found to be most interesting with numerous applications.[11] Plasmonics is based on excitation of surface plasmons (SP)—the collective oscillation of free electrons at metal dielectric interfaces due to optical interaction of matching frequency.[11−13] The plasmonic property of the metal nano structures varies from metal to metal, nanoparticle dimension, interparticle gap, and surrounding media of the nanostructure.[11,12] Plasmonic property of different metal−metal, metal insulator, metal oxide, metal inorganic semiconductor, and metal organic small conjugated molecule are studied and successfully applied in device realization.[12] Efficient plasmonic photosensitization of the conducting polymer has the ability to enhance the efficiency of organic photovoltaics.[14]

There are several recent reports on PAni-Au composite prepared mainly by chemical or electrochemical routes that explain enhanced catalytic activity[15] and are widely used in chemical as well as in biological sensors.[16] However, to the best of our knowledge, there is no report on the synthesis of PAni-Au composite by any type of dry process. There are verities of technologies available on dry synthesis of nanoparticles[17,18] but synthesis of conducting polymer metal nanocomposite thin film in dry environment is still a challenge. The beauty of the present work is in the synthesis of functional PAni-AuNP composite thin film deposition in dry environment and in single step process. Because this process is solvent free as well as water free, the process is environmentally friendly and the prepared material shows significantly higher stability.

In recent times, significant research works have been carried out that take advantage of novel plasma-based technology.[10,14] In our previous works, we have reported the exceptional stability of organic inorganic hybrid devices[6−8] prepared by plasma-based dry processing.

In this Letter, we present plasmonic photosensitization of a conducting polymer, which is PAni, and fabrication of a flexible hybrid photodetector based on PAni-AuNP composite film prepared by a single-step process using plasma polymerization in combination with pulsed DC magnetron sputtering. The as-fabricated plasmonic photodetector exhibits high speed, good

Received: November 17, 2014
Accepted: January 21, 2015
Published: January 21, 2015

DOI: 10.1021/am507821f
ACS Appl. Mater. Interfaces 2015, 7, 2166−2170

sensitivity and responsivity, very high detectivity, and high gain simultaneously with very low loading of AuNPs.

The details of the experimental procedure with a schematic of the deposition process is described in the Supporting Information (Figure S1). The fabricated hybrid photodetector has the configuration of PAni-Au/Ag-IDE/PET with a stacked structure of thickness 220 nm and lateral area of 8.6×10^{-6} cm^2. All the measurements of the hybrid photodetector are carried out after exposure of the device in the atmosphere and prepared nanocomposite is found to be stable upon months of exposure to air.

The schematic diagram and photograph of the photodetector fabricated over the flexible substrate are presented in panels a and b in Figure 1, respectively. From the Fourier transform

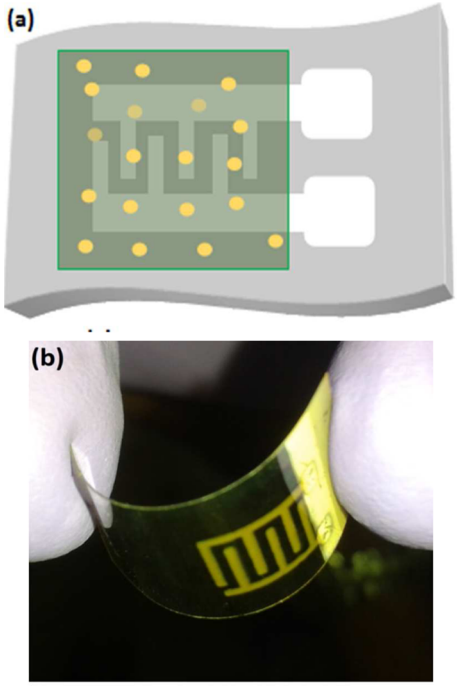

Figure 1. (a) Schematic of device structure of the PAni-AuNP composite-based flexible photodetector and (b) photograph of the photodetector.

infrared spectroscopy (see the Supporting Information, Figure S2) it is clear that the PAni is in the emerldine sequence, as it contains peaks due to benzenoid (1500 cm^{-1}) and quinoid (1600 cm^{-1}) units.[19] Additionally, the appearance of the intense sharp peak at 1107 cm^{-1} represents the doping of the PAni because of the incorporation of the gold nanoparticles. The chemical structure as well as doping of PAni due to the incorporation of Au-NP is further confirmed from the Raman spectroscopic analysis (see the Supporting Information, Figure S3). Similarly, in the UV−visible absorption spectroscopy (see the Supporting Information, Figure S4) the appearance of the absorption peak at 300 nm represents the $\pi-\pi^*$ transition on the benzenoid rings and the peak at about 600 nm appears due to plasmonic excitation of the conduction electron cloud of the gold nanoparticles. Transmission electron microscopic (TEM) and high-resolution transmission electron microscopic (HR-TEM) images are recorded at different magnifications to confirm the structure of the AuNP embedded in the polymer matrix (Figure 2a−d). From the HR-TEM images, it is clear that in the PAni-Au composite thin film, AuNPs of average size

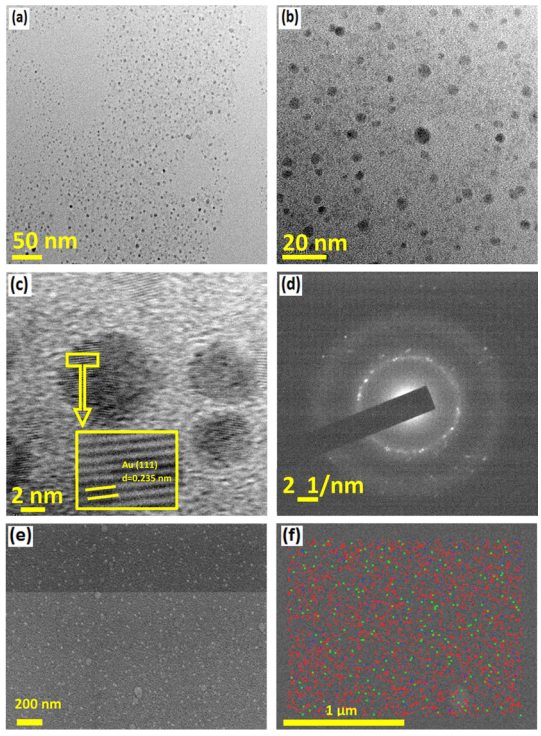

Figure 2. TEM images of PAni-AuNP composite at scale of (a) 50 and (b) 20 nm and HR-TEM image of PAni-AuNP composite at scale of (c) 2 nm. (d) SAED pattern of PAni-AuNP composite is presented. (e) FESEM image of the PAni-AuNP composite film and (f) EDX mapping image of the PAni-AuNP composite film, which reveals the uniform distribution of nanoparticles in the film.

of 5 nm are uniformly dispersed. The interplanar spacing of the (111) plane of the metallic AuNP is found to be 0.235 nm.[20] A clear diffraction pattern that is due to the presence of AuNPs in the selected area electron diffraction (SAED) image recorded using the HR-TEM further confirms the presence of the AuNPs in the deposited thin film. From the energy-dispersive X-ray (EDX) spectroscopic analysis (see the Supporting Information, Figure S5) it is confirmed that almost 1.5% Au is present in the polymer matrix. Further, in Figure 2e is presented a field-emission scanning electron microscopic (FESEM) image that clearly shows the uniformly dispersed nanoparticles on the uniform polymer film. EDX mapping image of the film is presented in Figure 2f, which reveals the distribution of AuNPs in the film.

Current versus voltage ($I-V$) characteristic of the Ag-IDE/PAni-AuNP device fabricated on the flexible PET substrate is recorded in the dark and under illumination of visible light of different intensities with a Keithley electrometer (6517B). The current of the Ag-IDE/PAni-AuNP device (Figure 3a) in dark is 1.49 μA at an applied voltage of 1.5 V, which increases to 166.80 μA when the device is illuminated by white light of intensity 72 mW/cm^2. The photocurrent of the current device displays strong dependence on the light intensity (see the Supporting Information, Figure S6a) and the corresponding light intensity versus photocurrent is plotted in Figure S6b in the Supporting Information, which can be fitted to a power law,[21] $I \sim P^{\theta}$, where θ determines the photocurrent response of the device to light intensity. The fitting shows slight deviation from linear behavior of light intensity dependence of photo current with $\theta = 0.95$.

DOI: 10.1021/am507821f
ACS Appl. Mater. Interfaces 2015, 7, 2166−2170

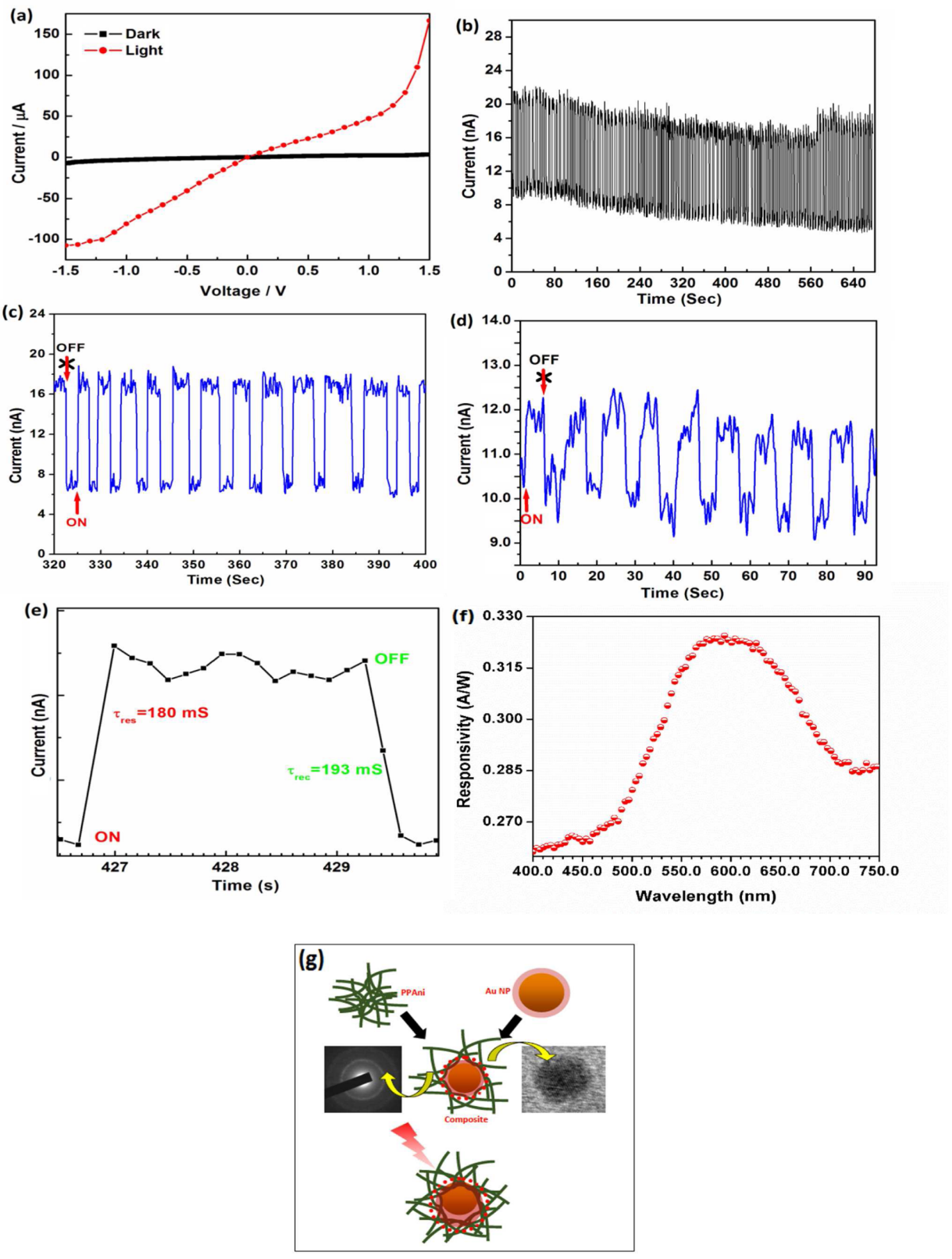

Figure 3. (a) *I*–*V* characteristics of the photodetector in the dark and under illuminations of white light. Reproducible on/off switching of the photodetector under illumination of white light (b) of intensity 72 mW/cm^2 and (c) magnified view, (d) of intensity 0.25 mW/cm^2. (e) Single-cycle on/off switching of the hybrid photodetector under illumination of white light. (f) Photoresponse vs wavelength spectra recorded under illumination of 3 μW of light and 1 V bias and (g) illustration for the charge transfer process within the Pani-AuNP composite. The electron cloud over the AuNP attracts positive charges from the PAni thus doping is achieved in the PAni. Light excites the collective SP oscillation of the free electrons of the AuNP and produces hot electrons because of the decay of the SP. These electrons are now capable of moving through the doped PAni.

DOI: 10.1021/am507821f
ACS Appl. Mater. Interfaces 2015, 7, 2166−2170

From the $I-V$ result, the photoconductance is calculated to be 111.2 μS under illumination of white light of intensity 72 mW/cm^2, and eventually the conductance decreases to 0.9 μS in the dark state. As illustrated in panels b and c in Figure 3, when the light was turned on and off alternately at a bias voltage of 1 V, the photodetector can be reversibly switched between low and high resistivity states, respectively. The reversible switching of the present photodetector is almost exactly reproducible for hundreds of on/off cycles, which represents the stability of the device.[9] The device is found to be sensitive even to a low intensity (0.25 mW/cm^2) LED flash light (Figure 3d).

Responsivity (R) of a photodetector is an important factor which reflects the electrical output per optical input of a photodetector, which is found to be 2.547×10^2 A W^{-1} for the present photodetector. Furthermore, to check the photoresponse of the hybrid photodetector, the photosensitivity (i.e., $(I_{light} - I_{dark})/I_{dark}$), is found to be 1.10×10^2. The photoconductive gain (G) is another key parameter to evaluate the sensitivity of photodetectors. The photoconductive gain is defined as the increase in the number of collected carrier per absorbed photon (with an energy $h\nu$). The photoconductive gain of the current photodetector is 5.092×10^2. The detectivity (D) of the photodetector is calculated and found to be 2.60×10^{14} Jones. The R, G ,and D values presented in this work are compared with few recently reported flexible photodetectors and are found to be superior in terms of detectivity and stability under repeated operation in ambient conditions.[8,10,22]

The applicability of the photodetector for using in the optical switching devices or optical communication systems is mainly depends on the speed. To determine the speed of the photodetector, we used the same electrometer to measure the time versus current at a fixed bias of 1 V under on/off states of visible light. The response time of a photodetector is defined as the time required in increasing the photocurrent from 10 to 90% and the recovery time is defined analogously.[6] Accordingly, 180 ms of the response and 193 ms of the recovery times are obtained for the current photodetector (Figure 3e), which is the limit of measurement of the Keithley electrometer used in this experiment. In Figure 3f, the responsivity versus wavelength spectra of the photodetector is recorded and the device shows maximum photoresponse at 600 nm which exactly corresponds to the UV−vis absorption spectra of the PAni-AuNP composite material (also see the Supporting Information, Figure S4).

Conductivity of pure polyaniline increases with incorporation of AuNPs. That is why we have noticed an increase in dark current of the device from 1×10^{-9} A to 1×10^{-6} A with incorporation of AuNPs. Under illumination of white light in the composite, the conductivity increases up to 1×10^{-4} A because of plasmonic photosensitization of the material. This is confirmed from the fact that pure polyaniline (without incorporation of Au) does not show any noticeable increase in conductivity under illumination because there is no photosensitization.

On the basis of the experimental data a simple mechanism of the device operation is proposed and schematically presented in Figure 3g. In the PAni-AuNP composite thin film, the PAni is in the emerldine base form, which is confirmed from the FTIR and Raman spectroscopy analyses. Because the loading of Au in the PAni matrix is only 1.5%, the enhancement of the conductance of the device under illumination of visible light is due to the charge transport through Pani as a result of plasmonic photosensitization. The AuNPs present in the polymer matrix have a free electron cloud over their surface. The electron cloud of the AuNPs attracts the positive holes from the PAni, thus PAni is doped, and therefore the conductivity of PAni increases under dark conditions when it is in the composite (Pani-AuNP) form.

When the PAni-AuNP composite is illuminated with light of matching frequency of SPs of AuNPs, hot electrons are generated[18] because of the decay of localized SPs of the AuNPs. These electrons are now freely movable through the doped PAni to the electrodes. Therefore, current flowing through the device in the presence of the light of matching frequency of the localized SP is significantly higher as compared to that in dark. So, doping and photosensitization of PAni is possible because of the incorporation of AuNPs.

In summary, we have successfully synthesized PAni-AuNP composite thin films in a single-step process, which show tremendous stability under ambient conditions. Based on the PAni-AuNP composite thin film a photodetector on flexible substrate is fabricated and the as-fabricated photodetector is found to be highly stable upon exposure to the atmosphere. The light-induced charge generation and transport in this hybrid material has been successfully evaluated, and a possible mechanism responsible for this charge transfer process has been proposed. The photodetector shows high sensitivity to visible light. The photodetector exhibited short response and recovery times (180 and 193 ms, respectively), enhanced photosensitivity (1×10^2), high photoconductive gain (5.092×10^2), high responsivity (2.547×10^2 AW^{-1}), and very high detectivity (2.60×10^{14} Jones). The merits of the present processing and device are (i) less time-consuming single-step solvent-free and water-free fabrication process, (ii) polymer-based plasmonic device with high stability in ambient conditions, (iii) flexible architecture, and (iv) good responsivity and speed, as well as very high detectivity. Overall, the study reveals the tremendous scope of the PAni-AuNP composite thin films prepared by this dry process for applications in the field of organic hybrid photodetectors.

■ ASSOCIATED CONTENT

Supporting Information

Detailed experimental methods, characterization of the PAni-AuNP composite thin film, preparation of Ag-IDE, device fabrication, and detailed electrical measurement results. This material is available free of charge via the Internet at http://pubs.acs.org

■ AUTHOR INFORMATION

Corresponding Author

*E-mail: arpal@iasst.gov.in. Tel.: +91 361 2912073. Fax: +91 361 2279909.

Notes

The authors declare no competing financial interest.

■ ACKNOWLEDGMENTS

This work was funded by the Institute of Advanced Study in Science and Technology (IASST), An Autonomous Research Institute of Department of Science & Technology, Government of India. The authors thank SAIF, NEHU, Shillong for providing the TEM and HR-TEM characterization facility.

DOI: 10.1021/am507821f
ACS Appl. Mater. Interfaces 2015, 7, 2166−2170

REFERENCES

(1) Chiang, J.-C.; MacDiarmid, A. G. 'Polyaniline': Protonic Acid Doping of the Emeraldine Form to the Metallic Regime. *Synth. Met.* **1986**, *13*, 193−205.

(2) Huang, W.-S.; Humphrey, B. D.; MacDiarmid, A. G. Polyaniline, a Novel Conducting Polymer. Morphology and Chemistry of its Oxidation and Reduction in Aqueous Electrolytes. *J. Chem. Soc., Faraday Trans.* **1986**, *82*, 2385−2400.

(3) Cao, Y.; Andreatta, A.; Heeger, A. J.; Smith, P. Influence of Chemical Polymerization Conditions on the Properties of Polyaniline. *Polymer* **1989**, *30*, 2305−2311.

(4) Quillard, S.; Louarn, G.; Lefrant, S.; MacDiarmid, A. G. Vibrational Analysis of Polyaniline: A Comparative Study of Leucoemeraldine, Emeraldine, and Pernigraniline Bases. *Phys. Rev. B* **1994**, *50*, 12496−12508.

(5) Wu, C.-G.; Bein, T. Conducting Polyaniline Filaments in a Mesoporous Channel Host. *Science* **1994**, *264*, 1757−1759.

(6) Hussain, A. A.; Pal, A. R.; Patil, D. S. An Efficient Fast Response and High-Gain Solar-Blind Flexible Ultraviolet Photodetector Employing Hybrid Geometry. *Appl. Phys. Lett.* **2014**, *104*, 193301−193304.

(7) Hussain, A. A.; Pal, A. R.; Patil, D. S. High Photosensitivity with Enhanced Photoelectrical Contribution in Hybrid Nanocomposite Flexible UV Photodetector. *Org. Electron.* **2014**, *15*, 2107−2115.

(8) Baro, M.; Hussain, A. A.; Pal, A. R. Enhanced Light Sensing Performance of a Hybrid Device Developed Using as-grown Vertically Aligned Multiwalled Carbon Nanotubes on TCO Substrates. *RSC Adv.* **2014**, *4*, 46970−46975.

(9) Fathalizadeh, A.; Pham, T.; Mickelson, W.; Zettl, A. Scaled Synthesis of Boron Nitride Nanotubes, Nanoribbons, and Nanococoons Using Direct Feedstock Injection into an Extended-Pressure, Inductively-Coupled Thermal Plasma. *Nano Lett.* **2014**, *14*, 4881−4886.

(10) Nguyen, K. T.; Li, D.; Borah, P.; Ma, X.; Liu, Z.; Zhu, L.; Grüner, G.; Xiong, Q.; Zhao, Y. Photoinduced Charge Transfer Within Polyaniline-Encapsulated Quantum Dots Decorated on Graphene. *ACS Appl. Mater. Interfaces* **2013**, *5*, 8105−8110.

(11) Mubeen, S.; Hernandez-Sosa, G.; Moses, D.; Lee, J.; Moskovits, M. Plasmonic Photosensitization of a Wide Band Gap Semiconductor: Converting Plasmons to Charge Carriers. *Nano Lett.* **2011**, *11*, 5548−5552.

(12) Tokel, O.; Inci, F.; Demirci, U. Advances in Plasmonic Technologies for Point of Care Applications. *Chem. Rev.* **2014**, *114*, 5728−5752.

(13) Ozbay, E. Plasmonics: Merging Photonics and Electronics at Nanoscale Dimensions. *Science* **2006**, *311*, 189−193.

(14) Gan, Q.; Bartoli, F. J.; Kafafi, Z. H. Plasmonic-Enhanced Organic Photovoltaics: Breaking the 10% Efficiency Barrier. *Adv. Mater.* **2013**, *25*, 2385−2396.

(15) Sharma, B.; Mandani, S.; Sarma, T. K. Enzymes as Bionanoreactors: Glucose Oxidase for the Synthesis of Catalytic Au Nanoparticles and Au Nanoparticle−Polyaniline. Nanocomposites. *J. Mater. Chem. B* **2014**, *2*, 4072−4079.

(16) Santhanam, V.; Andres, R. P. Microcontact Printing of Uniform Nanoparticle Arrays. *Nano Lett.* **2004**, *4*, 41−44.

(17) Park, C.; Lee, T.; Xia, Y.; Shin, T. J.; Myoung, J.; Jeong, U. Quick, Large-Area Assembly of a Single-Crystal Monolayer of Spherical Particles by Unidirectional Rubbing. *Adv. Mater.* **2014**, *26*, 4633−4638.

(18) Feng, X.; Zhang, Y.; Yan, Z.; Ma, Y.; Shen, Q.; Liu, X.; Fan, Q.; Wang, L.; Wei, H. Synthesis of Polyaniline/Au Composite Nanotubes and Their High Performance in the Detection of NADH. *J. Solid State Electrochem.* **2014**, *18*, 1717−1723.

(19) Barman, T.; Pal, A. R.; Chutia, J. Comparative Study of Structural and Optical Properties of Pulsed and RF Plasma Polymerized Aniline Films. *Appl. Surf. Sci.* **2014**, *313*, 286−292.

(20) Manjavacas, A.; Liu, J. G.; Kulkarni, V.; Nordlander, P. Plasmon-Induced Hot Carriers in Metallic Nanoparticles. *ACS Nano* **2014**, *8*, 7630−7638.

(21) Huo, N.; Yang, S.; Wei, Z.; Li, S.; Xia, J.; Li, J. Photoresponsive and Gas Sensing Field-Effect Transistors Based on Multilayer WS2 Nanoflakes. *Sci. Rep.* **2014**, *4*, 5201−5209.

(22) Wei, H.; Jin, G.; Wang, L.; Hao, L.; Na, T.; Wang, Y.; Tian, W.; Sun, H.; Zhang, H.; Wang, H.; Zhang, H.; Yang, B. Synthesis of a Water-Soluble Conjugated Polymer Based on Thiophene for an Aqueous-Processed Hybrid Photovoltaic and Photodetector Device. *Adv. Mater.* **2014**, *26*, 3655−3661.

DOI: 10.1021/am507821f
ACS Appl. Mater. Interfaces 2015, 7, 2166−2170